New Combining Rules for Rare Gas van der Waals Parameters

Marvin Waldman and A.T. Hagler*

Biosym Technologies, Inc., San Diego, California 92121

Received 23 October 1992; accepted 26 March 1993

New combining rules are proposed for the well depth, ε, and interaction distance, σ, describing nonbonded interatomic forces for rare gas pair interactions. Concepts underlying current combining rules applied in simulations of macromolecular and polymer systems are shown to be incompatible with experimental data on the rare gases. The current combining rules are compared with the new results using the experimental data. Mathematical properties of combining rules are considered, and it is shown how to reduce combining rule formulas from a two-parameter to a single-parameter problem. It is also shown how to graphically analyze combining rules against experimental data. We demonstrate using this analysis technique that the rare gas potentials do not obey a single combining rule for the ε parameter but do follow a single combining rule for the σ parameter. Finally, we demonstrate that a combining rule using both ε and σ can be used to predict the ε parameters for the mixed rare gas pairs.

INTRODUCTION

Understanding the nature of intermolecular forces is central to predicting both the microscopic and bulk properties of molecular systems. Molecular simulations involving molecular mechanics and dynamics calculations are often used to predict properties of interest such as structure, conformation, energy, transport coefficients, etc. of molecules ranging from peptide hormones and proteins to polymers.[1,2] These calculations rely on the use of force-field approximations for the quantitative description of the intra- and intermolecular forces. In most of the popular force fields in use, the description of the intermolecular component is broken down into contributions from electrostatic energy and a contribution from nonbond or van der Waal's interactions.[3-11] Due to the problem of overabundance of parameters, the nonbond interactions for unlike systems are generally approximated from knowledge of the interactions for like systems by the use of combining rules involving the nonbond parameters of the atom–atom pair potentials. The combining rules in common use with most available force fields are: (1) a geometric mean rule for the well depth parameter, ε, of the nonbond potential; and (2) a geometric or arithmetic mean rule for the well depth position, R_m, of the nonbond potential.[7]

In recent years, as experimental data provided more accurate information on nonbond potentials for rare gas interactions, it has become clear that these simple combining rules lead to large errors in predicting the potential parameters of mixed rare gas atom pairs, especially with regard to the well depth parameter, ε. As a result, more elaborate combination rules have been proposed that significantly improve the fit of the rare gas data, as well as other simple molecular systems.[12-15] However, none of these more elaborate rules have yet been incorporated into the more popular molecular mechanics force fields. In part, this may be due to the perception that the force fields are not sensitive to the specific form of the combining rules. However, another key factor is that the newer combination rules generally involve additional parameters such as polarizability, ionization potentials, or dispersion force coefficients. Therefore, these combination rules are less easily incorporated into molecular force fields because they lead, again, to an excess of parameters that are not easily determined for systems other than rare gases, and the original goal in employing combination rules was to reduce, rather than increase, the number of force-field parameters.

In this article, we propose new combination rules for the well depth and position parameters for nonbond potentials. These combination rules require no new parameters other than the values of the well depth and position themselves. We show how the new combining rules provide excellent fits to the well depths and interaction distances of the mixed rare gas pairs. Because of the specific data analyzed for the rare gas systems and for ease of comparison with prior work, we have actually chosen to use σ, the point at which the potential curve crosses zero, rather than R_m, the minimum of the curve, to for-

*Author to whom all correspondence should be addressed.

CCC 0192-8651/93/091077-08

mulate our distance parameter combination rule. Because it has been previously well established that the rare gas potentials follow a single reduced form in the region of the well to a good approximation,[16] a combining rule that holds for σ should also be equally valid for R_m.

As part of this study, we also demonstrate a method of graphically analyzing data for the purpose of elucidating possible combination rules. Through this analysis, we demonstrate that the rare gas atom pairs follow a combining rule in which the σ parameter for mixed systems depends only on the σ parameters for the corresponding like atom pairs. However, contrary to current thinking and application in most molecular simulations, the well depths, ε, do not follow a combining rule involving just the homonuclear εs. Instead, we obtain a suitable combining rule for the well depths through use of the quantity $\varepsilon\sigma^6$.

TESTING CURRENT COMBINATION RULES

In assessing combination rules for the rare gas pairs, an appropriate set of experimental or theoretical data with which to compare must first be chosen. We have chosen for our primary source for comparison the values for ε and σ obtained by Kestin et al.[16] in their corresponding states analysis of rare gas data (see Table A3 of their article). Although more recent potentials for the rare gas systems have appeared since then, they have involved different functional forms by different authors using different data. As such, we feel there is a greater likelihood that errors may be introduced when these potential parameters are compared to one another for the purpose of elucidating combination rules. The advantage of using the parameters of Kestin et al. is that all the data and functional forms were placed on an equal footing and analyzed in a consistent manner. Thus, while the individual values of ε and σ may not be the most absolutely accurate values in comparison with more recent data the nature of the corresponding states analysis used to obtain them helps make the values more internally consistent and, as such, more suitable for assessing combination rules. It is also important to note that *no combination rules were assumed or invoked to derive the parameters reported by Kestin et al.*

In Table I, we use the σ values of Kestin et al. to assess the performance of the arithmetic mean combination rule. The results in Table I illustrate the tendency of the arithmetic mean rule to systematically underestimate the σ values for the mixed rare gas pairs. Evidently, there is a tendency for the mixed value to lie closer to the larger of the two σs. We have not provided a direct comparison with the other popular combination rule for σ, the geometric mean, because we will show later that it exhibits a tendency

Table I. Test of arithmetic mean combining rule for σ. Upper right triangle is experimental data from Ref. 16. Lower left triangle is % error.

	He	Ne	Ar	Kr	Xe
He	2.610	2.691	3.084	3.267	3.533
Ne	*-0.3%*	2.755	3.119	3.264	3.488
Ar	*-3.4%*	*-2.1%*	3.350	3.464	3.660
Kr	*-5.4%*	*-3.1%*	*-0.1%*	3.571	3.753
Xe	*-8.1%*	*-4.8%*	*-1.2%*	*-0.7%*	3.885

Units in Å or, in italics, percent difference from experimental value.

$$\sigma_{ab} = \frac{1}{2}(\sigma_{aa} + \sigma_{bb})$$

to lie closer to the smaller of the two σs and hence performs more poorly than the arithmetic mean. The deficiency of the arithmetic mean combination rule has been noted by several other workers in the field who proposed various alternative combination rules for σ (or equivalently R_m).[12-15,17] In this article, we present an alternative rule that performs about equally well as the others but is particularly simple in form. In addition, we show that when used in conjunction with our new combination rule for ε it leads to further simplification and enables us to unify the ε, σ combination rules without the introduction of additional parameters such as polarizability, C_6 coefficients, or ionization potentials.

Before moving on to new combination rules, we close this section with an assessment of the geometric mean combination rule for ε, which is popularly employed in most force fields. In Table II, we see that it can result in large errors of over 50% in those systems containing very different well depths. In this case, the geometric mean systematically overestimates the well depths compared to the experimental values. Another interesting feature of the rare gas experimental well depths[16] is the apparent tendency to approach an approximately constant value for the He—(Ar,Kr,Xe) and Ne—(Ar,Kr,Xe) systems. In fact, contrary to what would be expected from current combination rules in molecular mechanics force fields, the (He,Ne)—Xe well depths are slightly smaller than the (He,Ne)—Kr well depths. Because

Table II. Test of geometric mean combining rule for ε. Same format as Table I.

	He	Ne	Ar	Kr	Xe
He	10.44	19.44	30.01	31.05	29.77
Ne	*7.7%*	42.00	64.17	67.32	67.25
Ar	*28.1%*	*20.2%*	141.5	165.8	182.6
Kr	*46.4%*	*35.4%*	*0.9%*	197.8	225.4
Xe	*79.7%*	*59.5%*	*7.8%*	*3.3%*	274.0

Units in °K or, in italics, percent difference from experimental value.

$$\varepsilon_{ab} = (\varepsilon_{aa}\,\varepsilon_{bb})^{1/2}$$

the Xe—Xe well depth is substantially larger than the Kr—Kr well depth, this raises the interesting question of whether a combination rule that is based solely on the values of the well depths can be found that quantitatively predicts this behavior. In the next section, we provide an analysis that attempts to answer this question.

MATHEMATICAL PROPERTIES OF COMBINATION RULES

There have been a number of studies involving combination rules for van der Waals nonbond parameters that assessed the performance of the various combination rules proposed based on the quality of their fits to rare gas and other data.[12-17] However, we are not aware of any studies that analyzed the data graphically to examine the deviations as well as to elucidate if a combination rule that fits the data was even possible. This is presumably the case because a combination rule generally predicts a single dependent variable (the well depth or distance for the mixed rare gas pair) from two independent variables (the well depths or distances for the homonuclear pairs). A graphical analysis would then seem to require a 3-D graph where along the x- and y-axes we represented the property (well depth or distance) for systems A—A and B—B respectively and along the z-axis we represented the experimental or predicted property for system A—B. This hardly seems a worthwhile exercise for the rare gases given that there are only 10 data points to graph, so that a numerical tabulation as we show in Tables I and II seems sufficient. However, seeking an understanding of trends and patterns in the data is generally better accomplished through a 1-D graphical analysis. These considerations motivated us to seek to reduce the apparent need for two independent variables to just one independent variable, which we now proceed to do via the following arguments.

Consider the general question of a property of a mixed system A—B that we denote by c (combined property). Let the corresponding properties for the pure systems A—A and B—B be denoted by a and b, respectively. We seek a function that predicts the value of c from knowledge of a and b. We call this function our "combination rule" for property c. Let us denote the function by $g(a, b)$. We then require

$$c = g(a, b) \tag{1}$$

What requirements can we infer for function g? For the kinds of properties in which we are interested, we make no distinction between systems A—B and B—A. Therefore, we require that g be a symmetric function:

$$g(a, b) = g(b, a) \tag{2}$$

Next, properties a, b, and c are always expressed in the same units. Our combination rule g must hold regardless of what unit system we choose for our property. Because different unit systems are related by a constant conversion factor, function g must be invariant to a uniform scaling of a, b, and c. Expressed as an equation, this means

$$sc = g(sa, sb) \tag{3}$$

or

$$sg(a, b) = g(sa, sb) \tag{4}$$

Combining the symmetry and scaling properties, we obtain

$$g(a, b) = ag(1, b/a) = ag(b/a, 1) \tag{5}$$

Let $r = b/a$. Further, let us define a new function, $f(r)$, as follows:

$$f(r) \equiv g(1, r) = g(r, 1) \tag{6}$$

Using eqs. (1) and (5), we can express $f(r)$ in terms of a and c:

$$f(r) = c/a \tag{7}$$

The importance of this result is as follows. If there is a combination rule g that can be used to predict property c from knowledge of a and b, and assuming g obeys eqs. (2) and (4), then the quantity c/a depends on the *single* variable $r(=b/a)$ through the function f. Therefore, if there is a valid combination rule g that correlates a, b, and c, *then a plot of* c/a *vs.* b/a *should lie on a single curve.* This curve is the function f. If we find, when we plot the data in this fashion, that it is scattered with no single curve that goes through all the points, then there is no combination rule that depends only on the pure system properties a and b that can be used to predict the mixed system property c for all the A—B systems considered. Of course, we always have to account for the possibility that experimental error may be the cause for failure of the points to lie on a single curve.

Now, let us consider the behavior of some of the more usual combination rules when expressed in this fashion. For example, the equation for the arithmetic mean rule is

$$c = (a + b)/2 \tag{8}$$

or

$$c/a = (1 + r)/2 \tag{9}$$

Similarly, the equation for the geometric mean rule is

$$c = (ab)^{1/2} \tag{10}$$

or

$$c/a = r^{1/2} \tag{11}$$

Therefore, if our data obey an arithmetic mean combining law, plotting c/a versus r should produce a set of points lying on a straight line with slope and intercept both equal to 1/2. Similarly, if a geometric mean combination rule is followed the plot of c/a versus r should yield a square root function.

Finally, to close this section we point out a few additional properties of the function $f(r.)$ We expect that if $a = b$ then the combination rule should predict that $c = b = a$. Mathematically, this corresponds to

$$g(a, a) = a \tag{12}$$

or

$$f(1) = 1 \tag{13}$$

Equation (13) will be termed the identity relationship. Returning to eq. (5) and reinvoking symmetry and scaling once more yields the following results:

$$g(a, b) = ag(1, r) = bg(1/r, 1) \tag{14}$$

or

$$f(r) = rf(1/r) \tag{15}$$

Equation (15) will be referred to as the reciprocity relationship. If we differentiate it with respect to r, we obtain another interesting property:

$$f'(r) = f(1/r) - f'(1/r)/r \tag{16}$$

Setting $r = 1$ and using eq. (13) yields

$$f'(1) = 1/2 \tag{17}$$

The significance of eqs. (13) and (17) is as follows. All combination rules will behave similarly in the vicinity of $r = 1$ ($a = b$) because the function $f(r)$ will have the same slope and intercept at $r = 1$ for all possible combination rules. Thus, to properly assess the performance of several alternative combination rules it is important to test their behavior for values of r significantly different from one.

In the next section, we perform an analysis of the rare gas data based on the ideas and equations presented above.

GRAPHICAL ANALYSIS OF RARE GAS DATA

We first examine the behavior of the rare gas σ values following the above treatment. In Figure 1, we plot the $\sigma_{bb}/\sigma_{aa}(r = b/a)$ values along the abscissa versus the $\sigma_{ab}/\sigma_{aa}(c/a)$ values on the ordinate. We have arbitrarily chosen σ_{aa} as the smaller number of the pair so that the abscissa values are always greater than one. The reciprocity relationship, eq. (15), justifies only examining values of r greater than one because we can obtain $f(1/r)$ from $f(r)$. In this figure, we also show the curves corresponding to the arithmetic mean rule, eq. (9), and geometric mean rule, eq. (11). It is clear, as we also found from the numerical analysis of Table I, that both of these standard rules systematically underestimate the actual experimental data. What the figure also clearly indicates is that the deviations from experiment grow as the ratio σ_{ab}/σ_{aa} increases, which was not clearly evident from Table I. Even more significant is that Figure 1 shows that the experimental data lie on a single curve (shown by the broken line) and, therefore, that the σ_{ab} values can be predicted from σ_{aa} and σ_{bb} by a single combination rule. Because it is clear from both Figure 1 and Table I that the arithmetic mean systematically underestimates the correct value of σ, we sought a combination rule that would be weighted toward the larger of the two σs. Such a combination rule can be obtained by using an average of a power (greater than one) of σ. We found that a sixth-power average fits the data well. This leads to the combination rule given by the following equation, which is shown as the broken line in Figure 1:

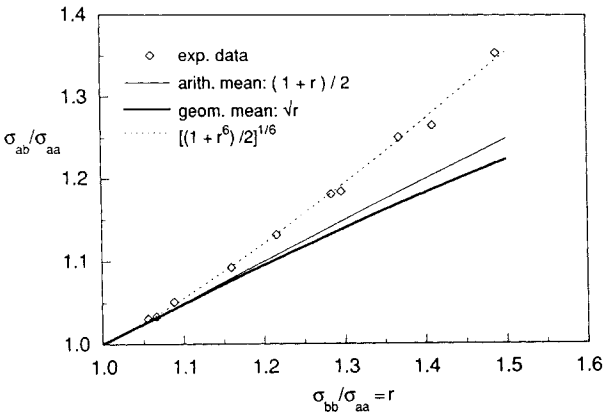

Figure 1. Graph of σ_{ab}/σ_{aa} versus σ_{bb}/σ_{aa} for experimental rare gas data from ref. 16. The thin solid line is arithmetic mean combination rule. The heavy solid line is geometric mean combination rule. The broken line is new sixth-power arithmetic mean combination rule.

$$f(r) = [(1 + r^6)/2]^{(1/6)} \tag{18}$$

or

$$\sigma_{ab} = \left(\frac{\sigma_{aa}^6 + \sigma_{bb}^6}{2}\right)^{1/6} \tag{19}$$

We have not used a least squares fit to obtain the sixth-power coefficient, so a slightly different value may provide a slightly better fit to the data, but we did not feel this was justified by the quality of the data. It is actually remarkable how well the simple sixth-power averaging performs. We show below how the value six helps simplify our proposed combining rule for ε, providing further justification for its use. In Table III, we demonstrate the quantitative accuracy of this new combination rule. We see that the errors have been reduced from a maximum deviation of 8.1% for the arithmetic mean rule to 1.2% for our sixth-power mean rule. In addition, the errors

Table III. Test of new combination rule for σ: Sixth power arithmetic mean. Same format as Table I.

	He	Ne	Ar	Kr	Xe
He	2.610	2.691	3.084	3.267	3.533
Ne	*-0.1%*	2.755	3.119	3.264	3.488
Ar	*0.1%*	*0.1%*	3.350	3.464	3.660
Kr	*-0.3%*	*0.6%*	*0.2%*	3.571	3.753
Xe	*-0.6%*	*1.2%*	*0.2%*	*-0.2%*	3.885

Units in Å or, in italics, percent difference from experimental value.

$$\sigma_{ab} = \left(\frac{\sigma_{aa}^6 + \sigma_{bb}^6}{2}\right)^{\frac{1}{6}}$$

are no longer systematic as can be clearly seen from both Figure 1 and Table III.

Next, we turn to a similar analysis of the experimental well depth data. In Figure 2, we plot the $\varepsilon_{ab}/\varepsilon_{aa}$ values versus $\varepsilon_{bb}/\varepsilon_{aa}$. In this case, ε_{aa} has been chosen as the larger of the two values so that the abscissa values are always less than one. We can see clearly that a single curve will not pass through all the points. In fact, it appears that there are two distinct curves formed by the points. These curves are drawn on the figure, but they are simply arbitrary interpolations of the data and have not been obtained from any equation. One curve seems to correlate the helium systems and another curve passes through the points for the nonhelium systems. It can also be seen that the geometric mean is systematically too high, and the arithmetic mean is even worse. The data would seem to indicate, therefore, that a single combination rule involving just the εs cannot be found that will correlate all the data. One possible solution would be to correlate the He systems with one rule and the non-He systems with a different rule. This would present some problems when trying to apply such rules to force-field parameterization schemes, and so we sought a different solution.

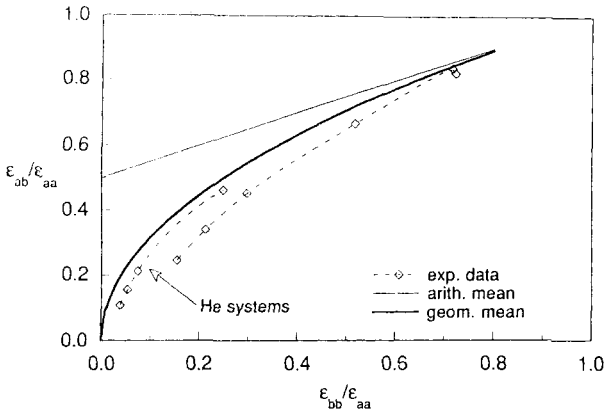

Figure 2. Graph of $\varepsilon_{ab}/\varepsilon_{aa}$ versus $\varepsilon_{bb}/\varepsilon_{aa}$ for experimental rare gas data from ref. 16. The two broken lines are arbitrarily drawn to illustrate the separation of the data for the helium and nonhelium systems.

In prior work, it has been noted that the quantity $\varepsilon\sigma^6$ may obey a geometric mean combination rule.[18-23] The idea arises by noting that for a Lennard–Jones potential $\varepsilon\sigma^6$ equals the long-range dispersion coefficient, C_6, and if a geometric mean rule is obeyed for C_6 it follows that $\varepsilon\sigma^6$ will obey such a rule.[18] Of course, the rare gas potentials are not really Lennard–Jones potentials and the C_6 coefficients do not obey a geometric mean all that closely.[16] Nevertheless, the suggestion has been investigated.[19-23] For example, DiPippo and Kestin[19] found that it was consistent with viscosity data while Van Heijningen et al.[20] showed it to be useful for correlating diffusion coefficients. In a later study, Lin and Robinson[21] found it to perform poorly with regard to second virial coefficient data. However, to properly employ it as a combination rule for ε also requires the use of a combination rule for σ. In previous studies by Lee and coworkers,[22,23] this was done by assuming the arithmetic mean combination rule for σ, and the results were found to be disappointing. More recently, little attention seems to have been paid to the geometric mean rule for $\varepsilon\sigma^6$ while more elaborate rules for ε have been devised.[12-14,17] In Table IV, we illustrate the performance of this combination rule for ε using the more recent data of Kestin et al.[16] and find the same level of performance as the earlier studies.[22,23] There is a mild improvement from the standard geometric mean combining rule for ε, but the largest error is still over 50%. However, the application of this rule is extremely sensitive to the rule employed for σ because it is raised to the sixth power in the formula, and this fact does not seem to have been previously noted.

Consequently, we have chosen to test the geometric mean rule for $\varepsilon\sigma^6$ in combination with our new sixth-power mean rule for σ itself. This leads to the following proposed combination rule for ε:

$$\varepsilon_{ab} = (\varepsilon_{aa}\varepsilon_{bb})^{1/2}\frac{2\sigma_{aa}^3\sigma_{bb}^3}{\sigma_{aa}^6 + \sigma_{bb}^6} \qquad (20)$$

Table IV. Test of geometric mean combining rule for $\varepsilon\sigma^6$ using arithmetic mean combining rule for σ. Same format as Table I.

	He	Ne	Ar	Kr	Xe
He	10.44	19.44	30.01	31.05	29.77
Ne	*7.5%*	42.00	64.17	67.32	67.25
Ar	*22.2%*	*16.7%*	141.5	165.8	182.6
Kr	*36.0%*	*28.7%*	*0.6%*	197.8	225.4
Xe	*59.7%*	*46.1%*	*6.1%*	*2.7%*	274.0

Units in °K or, in italics, percent difference from experimental value.

$$\varepsilon_{ab}\sigma_{ab}^6 = (\varepsilon_{aa}\sigma_{aa}^6\varepsilon_{bb}\sigma_{bb}^6)^{1/2}$$

$$\sigma_{ab} = 1/2\,(\sigma_{aa} + \sigma_{bb})$$

Table V. Test of geometric mean combining rule for $\varepsilon\sigma^6$ using new (sixth power arithmetic mean) combining rule for σ. Same format as Table I.

	He	Ne	Ar	Kr	Xe
He	10.44	19.44	30.01	31.05	29.77
Ne	*6.3%*	42.00	64.17	67.32	67.25
Ar	*-1.0%*	*2.1%*	141.5	165.8	182.6
Kr	*-0.8%*	*2.7%*	*-0.9%*	197.8	225.4
Xe	*-0.2%*	*0.9%*	*-2.0%*	*0.1%*	274.0

Units in °K or, in italics, percent difference from experimental value.

$$\varepsilon_{ab} = (\varepsilon_{aa}\,\varepsilon_{bb})^{1/2}\,\frac{2\,\sigma_{aa}^3\,\sigma_{bb}^3}{\sigma_{aa}^6 + \sigma_{bb}^6}$$

We see that use of eq. (19) has enabled simplification of the final formula for ε_{ab} resulting in eq. (20). In Table V, we assess the performance of this new rule. We see that it performs well with regard to the data with the worst error now being only 2.7% for the Ne—Kr system. Of course, this rule also suggests that a graphical analysis of the quantity $\varepsilon\sigma^6$ should produce a series of points that lie on a single curve when we plot $\varepsilon_{ab}(\sigma_{aa}^6 + \sigma_{bb}^6)/2\varepsilon_{aa}\sigma_{aa}^6$ versus $(\varepsilon_{bb}\sigma_{bb}^6)/(\varepsilon_{aa}\sigma_{aa}^6)$, where, in the first term, we substituted the combining rule formula from eq. (19) for the value σ_{ab}^6. In Figure 3, we show this plot for the rare gas data. It can be clearly seen that the data lie on a single curve over a wide range of values. Therefore, we conclude that $\varepsilon\sigma^6$ does obey a geometric mean combining rule for the rare gases when applied to the data of Kestin et al.[16] and that when used in conjunction with the sixth-power combining rule for σ forms an effective combining rule for the well depth parameter, ε.

SUMMARY

We assessed the performance of commonly used combination rules for van der Waals interaction parameters on rare gas data and found significant deviations when the arithmetic mean and geometric mean rules are used for σ and ε, respectively. Following a new graphical analysis of the data, we have shown that the sixth-power mean provides an excellent combination rule for σ. We have also shown that the well depths, ε, cannot be correlated by a combination rule involving only the εs. Instead, we found that a previously proposed combination rule using the geometric mean of $\varepsilon\sigma^6$ performs well when used in conjunction with our new combination rule for σ. The advantage of these combination rules over those previously proposed is that they correlate the data without the introduction of any additional parameters (such as dispersion force coefficients or polarizability) and are thus well suited for incorporation into molecular force fields, where the determination of such additional parameters is problematic. As Halgren also noted,[17] it still remains to be seen if combination rules derived from rare gas data will prove suitable for incorporation in molecular force fields in terms of their ability to fit molecular rather than rare gas data. Consequently, future articles based on this research will assess the performance of these combination rules with regard to their ability to fit experimental crystal data for small- to medium-size organic molecules.

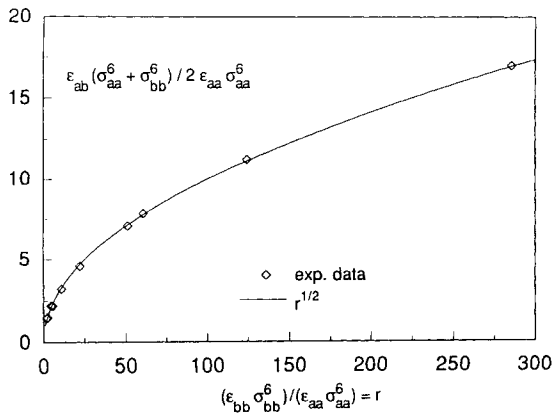

Figure 3. Graph of $(\varepsilon\sigma^6)_{ab}$ versus $(\varepsilon\sigma^6)_{aa}$ using experimental rare gas data from ref. 16 with σ_{ab} calculated from sixth-power arithmetic mean combination rule. The solid line is geometric mean combining rule for $\varepsilon\sigma^6$.

The authors thank Dr. Thomas Halgren for making a copy of his manuscript available to them prior to publication. This work was partially supported by the Consortium for Research and Development of Potential Energy Functions.

APPENDIX

As mentioned in the text, there is a variety of data available for the well depth and minima of the rare gases. Therefore, it is of some interest to compare our results using other data sets as a means of assessing sensitivity to the data and the influence of experimental error. Consequently, in this appendix we provide a comparison of the combination rules found in this work with other data sets and also with more recent combination rules that have proven effective in correlating the rare gas potential parameters.

In Tables A1–A6, we provide a comparison of our

Table A1. Combination rule comparison for σ using Halgren[17] data.

SYSTEM	EXPTL	PRESENT	TANG-TOENNIES	HALGREN
He-Ne	3.036	-0.3 %	0.2 %	-0.3 %
He-Ar	3.478	-0.2 %	0.6 %	-0.7 %
He-Kr	3.691	-0.7 %	0.0 %	-1.4 %
He-Xe	3.968	-0.5 %	0.0 %	-1.2 %
Ne-Ar	3.489	0.4 %	-0.3 %	-0.0 %
Ne-Kr	3.621	1.8 %	0.7 %	1.3 %
Ne-Xe	3.861	2.7 %	0.7 %	2.0 %
Ar-Kr	3.881	0.4 %	0.3 %	0.3 %
Ar-Xe	4.067	1.2 %	0.6 %	1.0 %
Kr-Xe	4.174	0.8 %	0.5 %	0.7 %
RMS		1.2 %	0.5 %	1.0 %

Table A2. Combination rule comparison for ε using Halgren[17] data.

SYSTEM	EXPTL	PRESENT	TANG-TOENNIES	HALGREN
He-Ne	20.89	2.2 %	-0.7 %	2.0 %
He-Ar	29.65	5.4 %	-1.0 %	6.7 %
He-Kr	29.50	10.2 %	2.5 %	11.0 %
He-Xe	28.00	13.3 %	4.1 %	11.7 %
Ne-Ar	67.59	-2.5 %	-1.9 %	-3.8 %
Ne-Kr	71.60	-2.9 %	-1.4 %	-5.0 %
Ne-Xe	74.20	-7.3 %	-4.6 %	-11.3 %
Ar-Kr	167.3	-0.5 %	-0.1 %	-0.4 %
Ar-Xe	188.6	-3.1 %	-0.5 %	-2.8 %
Kr-Xe	233.5	-1.2 %	-0.2 %	-1.0 %
RMS		6.3 %	2.3 %	6.9 %

Table A3. Combination rule comparison for σ using Tang–Toennies[14] data.

SYSTEM	EXPTL	PRESENT	TANG-TOENNIES	HALGREN
He-Ne	3.015	0.5 %	0.9 %	0.5 %
He-Ar	3.480	-0.2 %	0.6 %	-0.7 %
He-Kr	3.688	-0.6 %	0.1 %	-1.2 %
He-Xe	3.940	0.2 %	0.7 %	-0.5 %
Ne-Ar	3.417	2.5 %	1.8 %	2.1 %
Ne-Kr	3.630	1.6 %	0.4 %	1.0 %
Ne-Xe	3.870	2.4 %	0.5 %	1.7 %
Ar-Kr	3.881	0.4 %	0.3 %	0.3 %
Ar-Xe	4.067	1.2 %	0.6 %	1.0 %
Kr-Xe	4.174	0.8 %	0.5 %	0.7 %
RMS		1.3 %	0.8 %	1.1 %

Table A4. Combination rule comparison for ε using Tang–Toennies[14] data.

SYSTEM	EXPTL	PRESENT	TANG-TOENNIES	HALGREN
He-Ne	21.82	-2.8 %	-5.9 %	-3.4 %
He-Ar	29.80	4.5 %	-1.7 %	6.1 %
He-Kr	30.87	4.6 %	-1.8 %	6.5 %
He-Xe	30.00	5.4 %	-1.2 %	6.2 %
Ne-Ar	69.18	-4.7 %	-4.6 %	-6.4 %
Ne-Kr	70.70	-1.9 %	0.0 %	-3.7 %
Ne-Xe	72.20	-4.8 %	-0.5 %	-7.5 %
Ar-Kr	167.3	-0.8 %	-0.1 %	-0.5 %
Ar-Xe	188.6	-3.2 %	0.1 %	-2.2 %
Kr-Xe	233.5	-1.4 %	-0.2 %	-1.0 %
RMS		3.7 %	2.5 %	5.0 %

Table A5. Combination rule comparison for σ using Kestin[16] data.

SYSTEM	EXPTL	PRESENT	TANG-TOENNIES	HALGREN
He-Ne	2.691	-0.1 %	0.3 %	-0.2 %
He-Ar	3.084	0.1 %	0.8 %	-0.4 %
He-Kr	3.267	-0.3 %	0.3 %	-0.9 %
He-Xe	3.533	-0.6 %	-0.2 %	-1.3 %
Ne-Ar	3.119	0.1 %	-0.6 %	-0.3 %
Ne-Kr	3.264	0.6 %	-0.5 %	0.1 %
Ne-Xe	3.488	1.2 %	-0.7 %	0.5 %
Ar-Kr	3.464	0.2 %	0.0 %	0.1 %
Ar-Xe	3.660	0.2 %	-0.5 %	-0.1 %
Kr-Xe	3.753	-0.2 %	-0.5 %	-0.3 %
RMS		0.5 %	0.5 %	0.6 %

Table A6. Combination rule comparison for ε using Kestin[16] data.

SYSTEM	EXPTL	PRESENT	TANG-TOENNIES	HALGREN
He-Ne	19.44	6.3 %	2.8 %	5.8 %
He-Ar	30.01	-1.0 %	-6.9 %	0.2 %
He-Kr	31.05	-0.8 %	-7.6 %	-0.2 %
He-Xe	29.77	-0.2%	-7.7 %	-1.6 %
Ne-Ar	64.17	2.1 %	1.3 %	-0.6 %
Ne-Kr	67.32	2.7 %	2.7 %	-0.9 %
Ne-Xe	67.25	0.9 %	2.6 %	-4.7 %
Ar-Kr	165.8	-0.9 %	-0.4 %	-0.8 %
Ar-Xe	182.6	-2.0 %	0.9 %	-1.5 %
Kr-Xe	225.4	0.1 %	1.2 %	0.3 %
RMS		2.4 %	4.4 %	2.5 %

combination rules with the rules recently proposed by Tang and Toennies[14] and Halgren[17] using the data sets of Kestin et al.[16] based on the Law of Corresponding States analysis, the HFD potentials of Aziz and coworkers used by Tang and Toennies,[14] and the more recent set of literature HFD potentials used by Halgren. For comparison purposes, note that the σ values used by Halgren and Tang and Toennies actually correspond to the potential minimum (also referred to as R^*) whereas the σ values of the Kestin et al. data correspond to the potential zero crossing. Both the Halgren and Tang–Toennies combination rules require the additional input of homonuclear dispersion force coefficients, C_6, and atomic polarizabilities, α, which are used to generate heteronuclear C_6 coefficients via another combination rule. For the Tang–Toennies and Halgren data comparisons, we used the C_6 and α values as provided in their articles. For the Kestin data, we used the C_6 values in Table A5 of ref. 16 and the polarizability data used by Halgren.

Clearly, different assessments of the combination rules with respect to one another can be formed depending on the data set used for comparison. The Tang–Toennies rules are clearly superior for both ε and σ on the Halgren data set, whereas the Halgren and present rules appear to be superior for ε using the Kestin data set with all the rules performing about equally for σ on the Kestin data set. Actually, the difference between the performance of the Halgren and Tang–Toennies rules for ε on the Halgren data is surprising. This is because the two rules are in fact almost the same in that they are both based on assuming a geometric mean combination rule for $C_6^* = C_6/\varepsilon\sigma^6$. This can be seen most clearly from eqs. (33) and (34) of ref. 17:

$$\varepsilon_{ii} = \frac{1}{2} kG_i^2 C_{6ii}/R_{ii}^{*6} \tag{A1}$$

$$\varepsilon_{ij} = \frac{1}{2} kG_i G_j C_{6ij}/R_{ij}^{*6} \tag{A2}$$

Solving for G_i (and equivalently G_j) in eq. (A1) and substituting back into eq. (A2) yields

$$\varepsilon_{ij} = (\varepsilon_{ii}\varepsilon_{jj})^{1/2} \frac{R_{ii}^{*3} R_{jj}^{*3}}{R_{ij}^{*6}} \frac{C_{6ij}}{(C_{6ii}C_{6jj})^{1/2}} \tag{A3}$$

which is eq. (26) of ref. 14. The only difference between the two combination rules as employed by Halgren and Tang–Toennies is the different combination rules used for R_{ij}^* in the above formula (the combination rule used for C_{6ij} is the same). Thus, it is interesting that a factor of two difference in performance for σ between Tang–Toennies and Halgren leads to a factor of three degradation for ε. This results because R_{ij}^* is raised to the sixth power in the above formula (as well as the currently proposed combination rule). In fact, while we perform slightly poorer for σ compared to Halgren (using the Halgren

data), we perform somewhat better for ε. On the other hand, when using the Kestin data we and Halgren both do better than Tang–Toennies. Again, this is an interesting result because all the rules do about equally well for σ in this case.

These different assessments arise due to the sensitivity of the results on the input parameters and the presence of experimental error, especially for the heteronuclear εs. For example, our biggest error using the Halgren data is ε for He—Xe (13.3%). However, this sytem probably has the largest experimental error associated with it as it ranges between 28.0 used by Halgren to 30.0 used by Tang–Toennies. Overall, the heteronuclear εs are probably determined to within an error ranging from 5–10% and the σs probably have an error in the range of 1–2% using the differences in values from different researchers as a basis for making this estimate. Given this likely uncertainty in the numbers and the different assessments with different data, we feel it is not yet possible to make a definitive conclusion as to which combination rule performs best. We prefer our formulae because of the added simplicity of the equations and because *no additional experimental information other than ε and σ is required.* The latter point is especially important in using combination rules in force-field parameterization applications as has been recently pointed out by Hart and Rappé.[24]

References

1. A.T. Hagler, *The Peptides*, Ed. S. Udenfriend and J. Meienhofer, Vol. 7, 213 (1985).
2. R.-J. Roe, D. Rigby, H. Furuya, and H. Takeuchi, *Comp. Polym. Sci.*, **2,** 32 (1992).
3. N.L. Allinger, Y.H. Yuh, and J.-H. Lii, *J. Am. Chem. Soc.*, **111,** 8551 (1989).
4. S.J. Weiner, P.A. Kollman, D.T. Nguyen, and D.A. Case, *J. Comp. Chem.*, **7,** 230 (1986).
5. B.R. Brooks, R.E. Bruccoleri, B.D. Olafson, D.J. States, S. Swaminathan, and M. Karplus, *J. Comp. Chem.*, **4,** 187 (1983).
6. M.J. Sippl, G. Némethy, and H.A. Scheraga, *J. Phys. Chem.*, **88,** 6231 (1984).
7. A.T. Hagler, E. Huler, and S. Lifson, *J. Am. Chem. Soc.*, **96,** 5319 (1974).
8. S. Lifson, A.T. Hagler, and P.J. Dauber, *J. Am. Chem. Soc.*, **101,** 5111 (1979).
9 P. Dauber-Osguthorpe, V.A. Roberts, D.J. Osguthorpe, J. Wolff, M. Genest, and A.T. Hagler, *Proteins*, **4,** 31 (1988).
10. W.L. Jorgensen and C.J. Swenson, *J. Am. Chem. Soc.*, **107,** 1489 (1985).
11. J. Hermans, H.J.C. Berendson, W.F. van Gunsteren, and J.P.M. Postma, *Biopolymers*, **23,** 1513 (1984).
12. M.D. Peña, C. Pando, and J.A.R. Renuncio, *J. Chem. Phys.*, **76,** 325 (1981).
13. M.D. Peña, C. Pando, and J.A.R. Renuncio, *J. Chem. Phys.*, **76,** 333 (1981).
14. K.T. Tang and J.P. Toennies, *Z. Phys. D*, **1,** 91 (1986).
15. G. Ihm, M.W. Cole, F. Toigo, and J.R. Klein, *Phys. Rev. A*, **42,** 5244 (1990).
16. J. Kestin, K. Knierim, E.A. Mason, B. Najafi, S.T. Ro, and M. Waldman, *J. Phys. Chem. Ref. Data*, **13,** 229 (1984).
17. T.A. Halgren, *J. Am. Chem. Soc.*, **114,** 7827 (1992).
18. R. Reid and T.W. Leland Jr., *AIChE J.*, **11,** 228 (1965).
19. R. DiPippo and J. Kestin, *J. Chem. Phys.*, **49,** 2192 (1968).
20. R.J.J. Van Heijningen, J.P. Harpe, and J.J.M. Beenakker, *Physica*, **38,** 1 (1968).
21. H.-M. Lin and R.L. Robinson Jr., *J. Chem. Phys.*, **54,** 52 (1970).
22. C.H. Chen, P.E. Siska, and Y.T. Lee, *J. Chem. Phys.*, **59,** 601 (1973).
23. C.Y. Ng, Y.T. Lee, and J.A. Barker, *J. Chem. Phys.*, **61,** 1996 (1974).
24. J.R. Hart and A.K. Rappé, *J. Chem. Phys.*, **98,** 2492 (1993).